

Reliability of cascaded THz frequency chains with planar GaAs circuits

Frank Maiwald, Erich Schlecht, Robert Lin, John Ward, John Pearson, Peter Siegel, and Imran Mehdi

Jet Propulsion Laboratory, California Institute of Technology, MS 168-314, 4800 Oak Grove Drive, Pasadena, CA 91109

Abstract — Planar GaAs Schottky diodes will be utilized for all of the LO chains on the HIFI instrument for the Herschel Space Observatory. A better understanding of device degradation mechanisms is desirable in order to specify environmental and operational conditions that do not reduce device life times. Failures and degradation associated with ESD (Electrostatic Discharge), high temperatures, DC currents and RF induced current and heating have been investigated. The goal is to establish a procedure to obtain the safe operating range for a given frequency multiplier.

1. Introduction

Planar GaAs Schottky devices have been developed for fixed-tuned broadband frequency doublers and triplers [1-4] with output frequencies ranging from 140 to 1900 GHz for the Heterodyne Instrument for Far-Infrared (HIFI) on the Herschel Space Observatory (HSO). In order to obtain satisfactory amounts of RF power especially at the high end of this spectrum it is important to pump the first multiplier stage in a cascaded chain with 100-200 mW of power. These power levels are now available due to recent developments in W-band power amplifiers [5]. For instance, for a cascaded chain to 1200 GHz, the 200 GHz stage is pumped with 100 to 200 mW at WR-10 band, the 400 GHz stage with 30 to 50 mW, and the final stage with 3 to 10 mW. For the purpose of space qualification, a solid understanding of the risks associated with diode failures has to be achieved. Therefore, the reliability of planar GaAs Schottky diodes has been systematically investigated with the goal to define guidelines for determining the safe operating range of varactor diode frequency multipliers.

The work described in this paper is based on the investigation of various failure mechanisms that might occur in the device based on environmental and operational conditions. In most cases there is no redundancy in the LO chains and thus a failure of one device represents a single point failure causing that whole frequency band to be non-operational. It is also important to understand these failure mechanisms so that environmental and operational precautions can be appropriately placed to mitigate risk.

Failure mechanisms associated with ESD, high temperatures, and current (both DC and RF) have been investigated in some detail. Our investigations into these failure modes will now be presented in some detail, however, it should be kept in mind that the goal of this study is to establish a safe operating range for the HIFI diodes in particular and to establish some general procedures that can be used as guidelines for any given frequency multiplier.

2. Degradation due to Electrostatic Discharge (ESD)

ESD is perhaps the single most common failure mechanism in high frequency diodes. This is unfortunate since this risk is also quite easily mitigated by sound engineering procedures. For a quantitative analysis, the ESD susceptibility of five planar GaAs devices was measured in forward as well as in reverse bias for a number of different dopings. The ESD measurement was performed with a human body model (HBM) ESD simulator circuit, based on MIL-STD-883 Method 3015.7 [6]. The HBM is modeled by a 100 pF capacitor discharging through a switching device and a 1500 ohm resistor in series to the DUT (Device Under Test). The discharge produced a double exponential waveform with a rise time of 25 ns and a pulse-duration of approximately 250 ns. This test simulated the conditions when ESD sensitive hardware is handled without protection, such as proper grounding of operator and hardware. The ESD voltage pulse was increased in steps of 10 V or 20 V in the forward direction and -5 V or -10 V in the reverse direction. After each ESD pulse the diode voltage for $\pm 1 \mu\text{A}$ was measured. A failure was defined as a 10% change in this voltage in either direction.

A comparison between pulses in the forward and reverse direction indicated that the device is more susceptible to pulses in the reverse direction, consistent with results reported for large area Schottky diodes [7]. In forward a nominal diode can withstand ESD pulses that were 2 to 4 times higher than reverse. However, since it is impossible to predict the ESD pulse polarity the upper limit is taken to be the pulses in the reverse direction. The voltage magnitude that results in

damaging the diode (in reverse) for a number of different dopings is shown in Figure 1(a). After the failure of the device (as defined above), an inspection at 500x magnification of the individual anodes showed no visual evidence of damage. The damage to the device is probably based on localized heating under the anode metallization or metal migration. Since the devices are extremely sensitive to ESD, they have to be classified as Class I ESD Sensitive Devices per MIL-STD-883. In order to mitigate the ESD risk the implementation of sound engineering practices such as proper grounding, ESD safe working space and elimination of ground loops is highly recommended. A number of possible approaches can be used to reduce sensitivity to ESD [8].

A possible filter circuit that consists of two RC filters in series is shown in Figure 1 (b). The capacitors also help to reduce high frequency noise on the bias line. When biased through this circuit the diode was able to withstand ESD pulses up to 2000 V (upper limit reached by measurement apparatus), as shown in Figure 1(c).

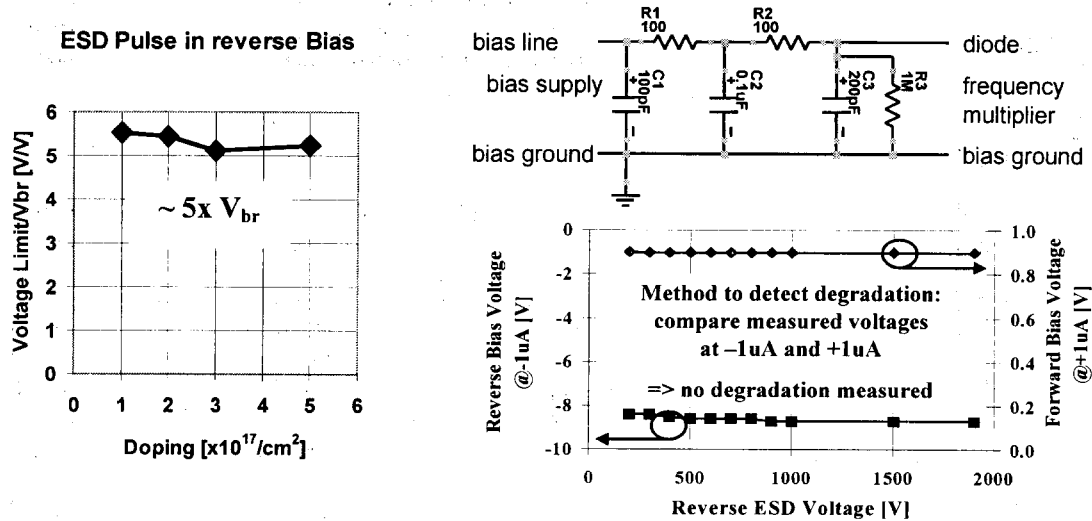


Figure 1: (a) ESD pulse magnitude in the reverse direction (normalized to the breakdown voltage) is plotted as a function of doping for onset of degradation. (b) The circuit diagram of the filter used to suppress ESD shock, and (c) the measured peak ESD pulse voltage for both positive and reverse directions when the ESD is applied through the protection circuit.

3. Temperature induced failures

Metal diffusion into the semiconductor can degrade diode performance. High temperature, high electric fields or a combination of the two can accelerate this process. Measuring times-to-failure for these devices at different temperatures does quantitative analysis of the thermally activated failures. The observed failure times are plotted on an Arrhenius plot allowing one to extrapolate mean-time-to-failure for any given operational temperature.

In earlier experiments, the activation energy of Schottky diodes was estimated to be between 0.6 to 1.2 eV [9]. Multiplier diodes from most recent batches were measured for mean-time-to-failure (MTTF) times by assuming an activation energy of 0.5 eV (to be on the conservative side). Results from this long-term failure test are plotted in Figure 2. The failure criteria was defined as change relative to the pre-test value of more than 15% of the ideality constant η , 20% of series resistance R_s , 20% of forward bias voltage at +1 μA , or 40% of reverse bias voltage at -1 μA . The mission lifetime specification for HIFI is about 1500 hours at ambient temperature of 120 K.

The MTTF measured for JPL Schottky diodes is 400 hours at 180°C, 200 hours at 200°C, and 100 hours at 240°C. However, it is important to state that these temperatures are assumed to be without the presence of any DC or RF power and are thus more akin to measuring the shelf life of the diodes. To determine more realistic operational MTTF times for these diodes it is important to determine the hottest point of the chip in the presence of RF power.

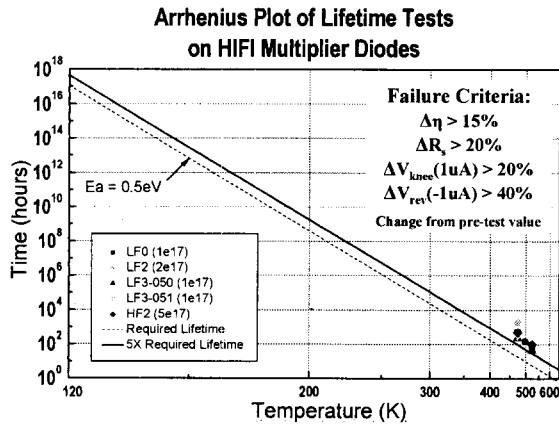


Figure 2: Measured MTTF of JPL diodes at 180C, 200C, and 240C.

A simple model was used to predict the heating of the chip due to RF [2]. This model is based on the topology of the diode chip and uses a temperature dependent thermal conductivity of GaAs, since GaAs devices are susceptible to thermal runaway problems. A preliminary verification of the diode thermal model was done by mounting a varactor device in a open waveguide block, biasing with DC currents that mimics RF induced heating and measuring the temperature rise of the chip via a recently available infrared camera with a spatial resolution of 2.8 μm (15x lens) [10]. This measurement closely matched our predicted results based on the simple model.

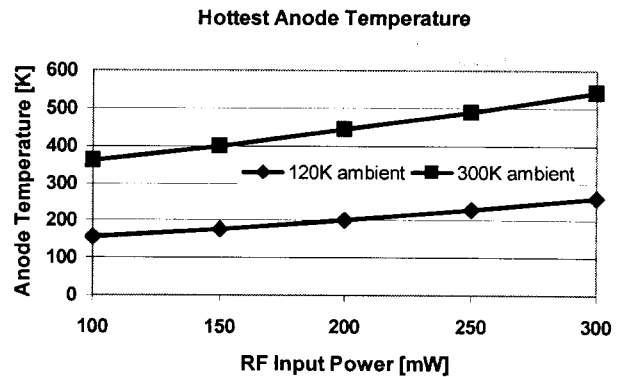
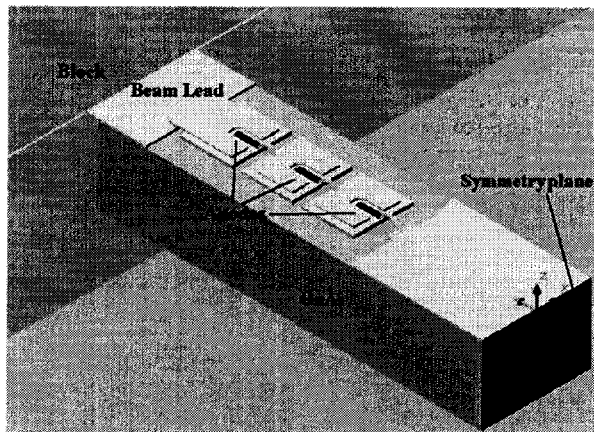


Figure 3: Schematic of one-half of a nominal 200 GHz doubler chip used for the thermal analysis. The predicted temperature of the hottest anode on the chip is plotted as a function of input power. The multiplier is assumed to be 25% efficient in converting the input power to the output power. It was assumed that the rest of the power is dissipated equally by the six anodes on the chip.

Based on the simple model one can now determine the operational lifetime of the diodes based on the hottest temperature point on the chip. For 150 mW of pump power the hottest anode temperature is determined to be 400 K when the block temperature is at room temperature. This would indicate that the expected lifetime would be ~ 300 days. However, when the block temperature is set to 120 K (operational temperature for HIFI) the expected temperature of the hottest anode is only 177 K assuming 150 mW of input power. This would indicate that the lifetime of the diodes would be in excess of 1 million years, significantly higher than the mission lifetime.

Use of the MTTF given from the Arrhenius plot is helpful in increasing the confidence that one can place in the integrity of the device fabrication process. Process degradations such as lack of diffusion barriers, impurities, and infant mortality can be exposed by such experiments. However, accurate device thermal modeling is needed to determine the actual device temperature and this should be used to extrapolate the MTTF for the given device.

4. DC current induced damage

DC current-voltage characteristics are the most widely used health check for Schottky diodes. However, it is often not obvious what current maximums can be applied without fear of degradation. For each wafer lot, five devices were selected for the forward current ramp test, and five additional devices for the reverse current ramp test. For each device the I-V characteristic was measured before each incremental step in the current ramp. The current was iteratively increased by 0.5 mA in forward and by 0.010 mA in reverse with a dwell time of 2 minutes. The test continued until a catastrophic failure was detected. The failure was defined by a change of more than 50% on any of the DC parameters, i.e., ideality factor η , series resistance R_s , turn-on or forward voltage $V_f(1 \mu\text{A})$, and reverse voltage $V_r(-1 \mu\text{A})$.

The current density resulting in diode failure in the forward direction is shown in Figure 4(a) as a function of doping. The current density increases drastically with doping. The measured maximum of the forward DC current is limited by the diode's ability to dissipate heat. Bias conditions below these limits guarantee that the diode will not be damaged. To be safe, the highest nominal current density in the forward bias direction was selected as $0.5 \text{ mA}/\mu\text{m}^2$ which is about 10 times lower than the value that results in damage. It is also highly recommended that the I(V) curve of the diode be measured in a pulsed mode to avoid the measurement being tainted by self heating.

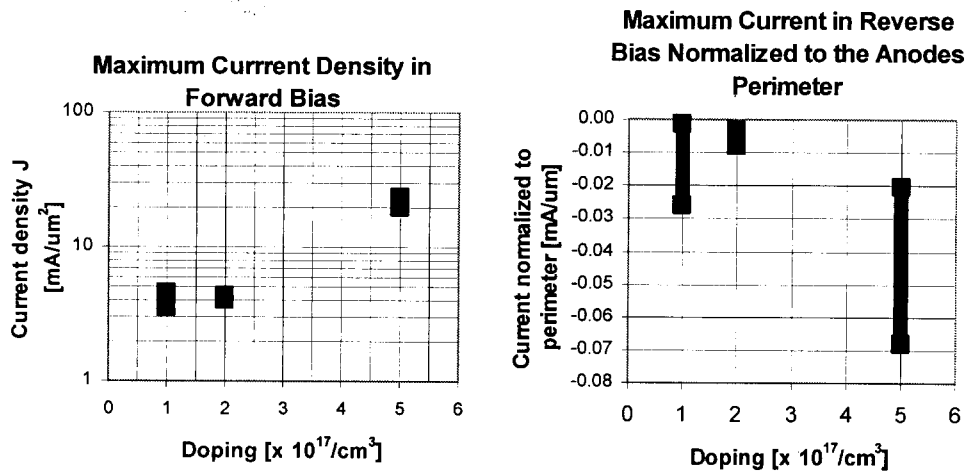


Figure 4: (left) The current density in the forward direction that results in device degradation is plotted as a function of doping. (right) The reverse current that results in degradation is plotted normalized with respect to diode periphery. In both cases multiple data points are measured for each doping.

In the reverse direction, due to the high electric field it is expected that most of the current will pass through the diode periphery rather than the diode area. This was confirmed by matching the actual measured reverse currents to a thermionic emission model that takes into consideration the current through the diode periphery. This phenomenon is also well documented for FET devices [11] and GaAs diodes [12]. The current per unit periphery for different dopings is shown in Figure 4(b). The large variation in the measured diode indicates that perhaps the microscopic interface between the diode periphery and GaAs has more of an effect than the doping of the epilayer. Even small amounts of currents in the reverse direction can permanently alter the device I(V). However, breakdown voltage is often quoted as an important device characteristic and it is necessary to pass reverse current to measure this voltage. It has been shown that the device I(V) is

sensitive to both the magnitude as well as the duration of the reverse current [13], thus it is recommended to define the breakdown voltage for very small reverse currents (less than $0.01\text{mA}/\mu\text{m}$) and to not excessively measure the breakdown voltage for a given anode. This degradation is probably due to the presence of traps at the GaAs/passivation interface. A calculated potential profile for an anode under reverse bias shows high electric fields at the edge which can cause energetic electrons to create traps at the interface. Impact ionization from electrons accelerated in the high field produces high-energy holes and electrons that can also be trapped near the nitride/GaAs interface.

5. RF induced failures and the determination of the safe operating range

In order to understand failure modes associated with the application of RF power it is instructional to visualize the different RF induced currents and voltages present in a multiplier when it is being pumped. A harmonic balance simulation coupled with a 3-D electromagnetic simulator can be used to determine the various currents in a given multiplier. A nominal case is presented in Figure 5. A 200 GHz anode with a breakdown voltage of 10.4 V and 25 mW of input power is assumed. The various currents in the diode, forward current peak ($I_{\text{peak fwd}}$), reverse current peak ($I_{\text{peak rev}}$), forward average ($I_{\text{avg fwd}}$) and reverse average ($I_{\text{avg rev}}$) currents along with the calculated diode efficiency (%) are plotted. Moreover, the reverse peak bias voltage ($V_{\text{peak rev}}$) is also plotted. For high efficiency operation the calculated reverse voltage peaks approaches close to the breakdown voltage, resulting in a large reverse current peak. While the bias voltage and average bias current are measurable, there is no easy way of measuring the reverse and forward peak currents. Simulations such as these are highly dependent on the circuit design and strongly frequency dependent. Multipliers can also be designed to be optimally biased further away from the breakdown voltage, but in order to obtain higher output power; the design simulated in Figure 5 is more typical.

Determining the safe operating zone for a given multiplier boils down to finding the bias range where no significant reverse current is present. The following procedure can be used to determine the safe operating range. A multiplier is biased at a reverse bias voltage and the coupled RF input power to the diode is increased monotonically. When the measured bias current indicates a value of $-5\ \mu\text{A}$ in the reverse direction the bias conditions and the coupled power are recorded and the RF power is reduced to zero. The coupled power can be measured with a bi-directional waveguide coupler. Next a slightly more positive bias voltage is selected and the input power is again increased slowly to determine the coupled power and bias voltage for $-5\ \mu\text{A}$ of current. This process is repeated for a number of bias values. Then the bias voltage is plotted with respect to the square root of the coupled power. Such a plot is shown in Figure 6.

The linear like behavior of the coupled power with the bias voltage allows one to extrapolate the data. With 100 mW of coupled power the bias voltage is approximately $-11\ \text{V}$. However, at this bias voltage the measured bias current is $-5\ \mu\text{A}$ indicating that the reverse bias current peak is probably closer to $-50\ \mu\text{A}$. Such a large reverse current peak is not suitable for long-term operation since cumulative degradation has been shown for reverse constant current stress [13, 14]. Thus the recommended bias voltage is derated by approximately 25% to $-8\ \text{V}$. This is also close to the optimum bias voltage. The limit of $-8\ \text{V}$ was set to ensure that the operation is within the safe bias range with power levels up to 100 mW. This establishes the envelope of the maximum reverse bias voltage to eliminate risk due to the large reverse peak current. In the forward direction the envelope is determined by the maximum current that can be sustained by the diode with damage as discussed earlier (approximately $0.5\text{mA}/\mu\text{m}^2$). Thus, between these two boundary conditions lies the safe operating zone of this particular multiplier.

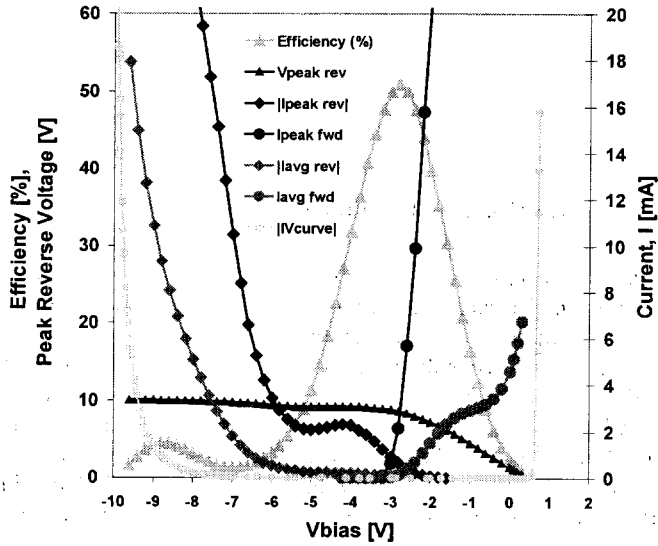


Figure 5: Simulation of a 200 GHz doubler with 25 mW of input power (breakdown voltage is 10.4 V). Multiplier efficiency and various currents through the diode are depicted.

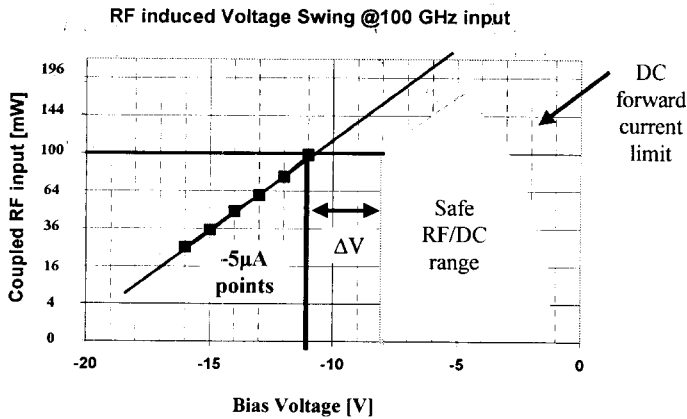


Figure 6: Proposed procedure for determining the safe operating range of a 200 GHz doubler. The bias voltage is plotted as the square of coupled power for $-5 \mu\text{A}$ of reverse current.

CONCLUSION

A comprehensive reliability study of planar GaAs diodes with relatively high RF power capability has been conducted. ESD, high temperature, DC, and RF induced failures have been investigated. It has been shown that failure risk due to ESD, temperature, and DC currents can be substantially mitigated by proper engineering procedures. Failures due to excessive RF induced currents are intimately related to the circuit design and the magnitude of the RF induced peak reverse

current is difficult to measure directly. A general procedure has been proposed that is based on monitoring the bias current of the multiplier and then derating the bias voltage to reduce the reverse current through the anode. By following these guidelines one can ensure that the multiplier diodes operate in a safe zone where failure risks have been reduced.

ACKNOWLEDGEMENTS

We thank Neal Erickson (U-Mass) and Goutam Chattopadhyay (Caltech) for many fruitful discussions and insights regarding high frequency multiplier behavior. The team at MPIfR (Max Planck Institut fuer Radioastronomie) in Bonn, Germany for fruitful discussions and providing filter circuits. Ronald Ruiz (JPL) helped perform the measurements with the IR camera. Further we appreciated the huge support by the Submillimeter-Wave Advanced Technology Group (SWAT), especially the contributions of Raymond Tsang, Bradley Finamore, William Chun, and Alejandro Peralta. This work was performed at the Jet Propulsion Laboratory, California Institute of Technology, under a contract with the National Aeronautics and Space Administration (NASA).

REFERENCES

1. Neal Erickson, "Diode Frequency Multiplier for THz Local Oscillator Applications," *SPIE Conference on Advanced Technology MMW, Radio and Terahertz Telescopes*, SPIE Vol. 3357, pp. 75-84, March 1998.
2. E. Schlecht, G. Chattopadhyay, A. Maestrini, A. Fung, S. Martin, D. Pukala, J. Bruston and I. Mehdi, "200, 400 and 800 GHz Schottky Diode 'Substrateless' Multipliers: Design and Results," *2001 Int. Microwave Symp. Digest*, Phoenix, AZ, May 2001.
3. G. Chattopadhyay, E. Schlecht, J. Ward, J. Gill, H. Javadi, F. Maiwald, and I. Mehdi, "An All Solid-State Broadband Frequency Multiplier Chain at 1500 GHz," *IEEE Trans. On Microwave Theory and Tech.*, Vol. 52, No. 5, May 2004, pp. 1538-1547.
4. Alain Maestrini, John Ward, John Gill, Goutam Chattopadhyay, Frank Maiwald, Katherine Ellis, Hamid Javadi, and Imran Mehdi, "A Planar-Diode Frequency Tripler at 1.9THz," *IEEE MTT-S Int. Microwave Symp.*, Philadelphia, Pennsylvania, June 13, 2003.
5. L. A. Samoska, T. C. Gaier, A. Peralta, S. Weinreb, J. Bruston, I. Mehdi, Y. Chen, H. H. Liao, M. Nishimoto, R. Lai, H. Wang, and Y. C. Leong, "MMIC power amplifiers as local oscillator drivers for FIRST," *Proc. SPIE*, vol. 4013, San Diego, CA, Aug. 2000, pp. 275-284.
6. Sponsor: Surge-Protection Devices Committee of the IEEE Power Engineering Society, "IEEE Guide on Electrostatic Discharge (ESD): ESD Withstand Capability Evaluation Methods for Electronic Equipment Subassemblies," *IEEE Standards Board*, approved October 24, 1994.
7. Y. Anand, R.J. Malik, "Electrostatic Failure of GaAs Planar Doped Barrier Diodes," *EOS/ESD Symp.* 93-1003.
8. J.E. Vinson, J.J. Liou, "Electrostatic Discharge in Semiconductor Devices: Protection Techniques," *Proc. of the IEEE*, Vol. 88, No. 12, December 2000.
9. R. Lin, A. Pease, R. Dengler, D. Humphrey, T. Lee, S. Kayali, I. Mehdi, "Quartz-based GaAs Schottky Diodes - Lifetime and Failure Analysis," *Proc. of the 9th Int. Symp. on Space Terahertz Technology*, pp. 511-520, March 1998.
10. Quantum Focus Instrument Corporation (QFI), Denman D. Kessler at QFI.
11. S. Takatani, H. Matsumoto, J. Shigeta, K. Ohshika, T. Yamashita, and M. Fukui, "Generation Mechanism of Gate Leakage Current to Reverse-Voltage Stress in i-AlGaAs/n-GaAs HIGFET's," *IEEE Trans. On Electron Devices*, Vol. 45, No. 1, January 1998, pp. 14-20.
12. P. Dodd, T.B. Stellweg, M.R. Melloch, and M.S. Lundstrom, "Surface and Perimeter Recombination in GaAs Diodes: An Experimental and Theoretical Investigation," *IEEE Trans. On Electron Devices*, Vol. 38, No. 6, June 1991, pp. 1253-1261.
13. Frank Maiwald, Erich Schlecht, John Ward, Robert Lin, Rosa Leon, John Pearson, and Imran Mehdi, "Design and operational considerations for robust planar GaAs varactors: A reliability study," *Int. Symp. on Space THz Technology*, Tucson, April 22, 2003.
14. M. Schuessler, V. Krozer, K.H. Bock, M. Brandt, L. Vecci, R. Losi, and H.L. Hartnagel, "Pulsed Stress Reliability Investigations of Schottky Diodes and HBTS," *Pergamon, Microelectron. Reliab.* Vol. 36, No. 11/12, pp. 1907-1910, 1996